Time Resolved Diagnostics for Kinetic Studies in N2/O2 Pulsed rf Discharges

S. de Benedictis, G. Dilecce

Time Resolved Diagnostics for Kinetic Studies in N_2/O_2 Pulsed rf Discharges

S. De Benedictis (*) and G. Dilecce

Centro di Studio per la Chimica dei Plasmi C.N.R., c/o Dipartimento di Chimica Università di Bari, Via Orabona 4, 70126 Bari, Italy

(Received 7 February 1996, revised 5 April 1996, accepted 29 April 1996)

PACS.52.70.-m – Plasma diagnostic techniques and instrumentation
PACS.52.20.Hv – Atomic, molecular, ion, and heavy-particle collisions
PACS.52.80.-s – Electric discharges

Abstract. — Time resolved optical diagnostics have been applied to the study of energy transfers in N_2/O_2 pulsed radio-frequency discharge. $N_2(A^3\Sigma_u^+)$ and $NO(X^2\Pi)$ have been measured by Laser Induced Fluorescence, and NO-γ band by Emission Spectroscopy. The analysis in discharge and post discharge as a function of O_2 percentage allows to guess the main mechanisms correlating the relaxation of these species in the post-discharge. NO-γ bands in N_2/O_2 discharge are mainly excited by $N_2(A) + NO(X)$ collisions. The decay rates of $N_2(A)$ can be accounted for by O, NO and O_2 quenching. NO ground state density, measured by LIF, varies with O_2 percentages showing a bell shape profile with a broad maximum. Some EEDF measured by Langmuir probe under continuous discharge conditions show that O_2 addition, even in few percents, strongly reduces the density of low energy electrons.

1. Introduction

In our recent work on energy transfer processes in He-N_2 and He-O_2 plasmas [1,2], the use of pulsed discharges and time resolved diagnostics was emphasized as a very useful approach to the study of elementary processes under non-equilibrium plasma conditions. Time Resolved Plasma Induced Emission Spectroscopy (TRPIES) and Laser Induced Fluorescence (LIF) were employed for detecting during the pulsing of the discharge atomic and molecular species in radiative and metastable states, as well as time resolved Langmuir probe for measuring the Electron Energy Distribution Function (EEDF) in afterglow. The relaxation of the plasma in the early afterglow time offered a very useful complementary picture of the interplay of various excitation processes taking place during the discharge regime [3].

Actually we are interested in the reaction kinetics and energy transfers in N_2/O_2 discharges, and it is our opinion that the pulsing of the discharge and the use of time resolved diagnostics will improve the knowledge of such kinetics, the complexity of which is well-known under non equilibrium plasma conditions [4]. Electrons, metastable species and vibrationally excited molecules can, in fact, participate to the dissociation of N_2 and O_2 and to the formation of

(*) Author for correspondence.

O, N, NO, N_2O, NO_2 products [5–7]. The interest of many of these elementary reactions in the physical chemistry of upper atmosphere is well known and many papers have been devoted to their study [8]. On the other hand, the importance of non-equilibrium kinetics in N_2/O_2 mixtures has been recently emphasized in the study of the reactivity encountered under re-entry conditions of hypersonic vehicles [9,10].

Our investigations have been carried out in a low pressure N_2/O_2 pulsed parallel plate radio frequency discharge. Such device extends the interest of N_2/O_2 non equilibrium kinetics to technological applications in materials deposition and/or treatment carried out under afterglow conditions [11]. We have at present measured $N_2(A^3\Sigma_u^+)$ metastable and NO, that are only few of the most important species involved in N_2/O_2 kinetics. In the present paper we will mainly focus on the use of LIF spectroscopy for detecting NO ground and $N_2(A^3\Sigma_u^+)$ metastable and on TRPIES for detecting NO-γ bands. We will see that the measure of NO density and the analysis of the decays of $N_2(A, v = 0)$ and NO-γ band by varying the amount of O_2 in the feeding mixture, allow to stress the prevailing mechanisms of $N_2(A)$ quenching and NO-γ bands excitation under plasma conditions and, finally, to infer some features of the O_2 dissociation. Some Langmuir probe measurements of EEDF in rf discharge under continuous excitation condition (cw), offer the basis for a qualitative discussion of O_2 role in the electron kinetics.

2. Experimental

The block scheme of the experimental set-up indicating the various diagnostic facilities is shown in Figure 1. Here we recall some features important for N_2/O_2 experiments. More details can be found elsewhere [1,2].

2.1. Plasma Device. — The discharge is produced in a parallel plate reactor. Both the vacuum and the electrodes are stainless steel. The discharge is confined inside the 5 cm electrode gap. The 27 MHz rf generator has been pulsed at 100 Hz and 50% duty cycle. The N_2/O_2 mixtures are prepared by calibrated flows of N_2 and O_2. Static pumping of the chamber is achieved by a diffusion pump equipped with a LN_2 cold trap. The leak rate of the chamber plus the gas feeding lines is about 7×10^{-5} Torr litre^{-1} s^{-1} The dynamic pumping is maintained by a rotary pump. The pressure inside the chamber is measured by a capacitance manometer and is regulated during the experiments by a valve on the pumping line. The present experiments have been carried out at 0.1 Torr total pressure and 60 W discharge power (measured under continuous, cw, operation). The partial pressure of O_2 has been varied from 1% to 95%. The total flow rate has been maintained in most conditions at 80 sccm.

2.2. Diagnostics. — The experiments are executed under computer control. Discharge pulsing, laser firing, and detection facilities are synchronously driven by a master trigger. The delays of the laser pulse and of data acquisition can be varied with respect to the discharge pulse. This allows the measure of relaxation of the species during the discharge and post-discharge. The repetition rate of the laser is 10 Hz, while the discharge can be pulsed with variable frequency and duty cycle. In the present experiments, the discharge frequençy has been fixed to 100 Hz with 50% duty cycle.

All the spectroscopic measurements have been carried out on the rf discharge with one electrode dc coupled to the power supply and the other one grounded (symmetric configuration). The radiation from the discharge is sampled perpendicularly to the axis of the chamber by a couple of lenses with magnification $M = 1$.

2.2.1. $N_2(A, v)$ *Detection.* — LIF detection of $N_2(A, v = 0, 5, 7)$ levels has been achieved by the excitation-detection of $N_2(B^3\Pi_g - A^3\Sigma_u^+)$ First Positive band System (FPS). Excitation

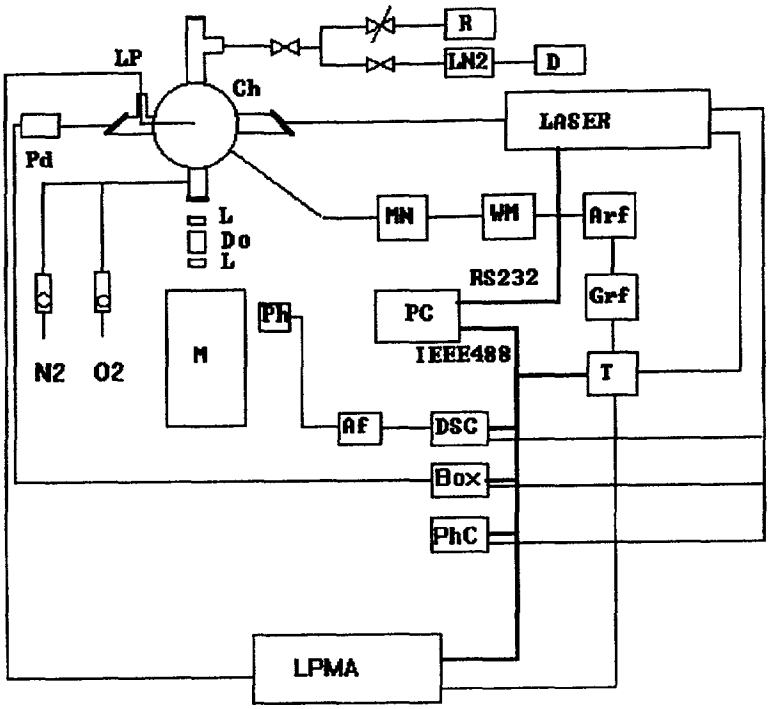

Fig. 1. — Experimental set-up currently employed in our laboratory for the measurement of the metastable states, radiative species and electrons. Af: fast amplifier; Arf: wide band rf power amplifier; Box: boxcar amplifier; Ch: vacuum Chamber; D: Diffusion pump; DSC: digitizing O-scope; Do: Dove prism; Grf: low power rf Generator; L: Lens; L N_2: Liquid Nitrogen trap; Lp: Langmuir probe; LPMA: Langmuir Probe Measurement Apparatus; M: Monochromator; MN: Matching Network; PC: Personal Computer; Pd: Photodetector; Ph: Photomultiplier; PhC: Photon Counter; R: Rotary pump; T: Timing cards; WM: wattmeter.

occurs by a 0.2 cm^{-1} Nd-Yag pumped dye laser tuned close to the P11 band head of each transition [12]. Detection takes place by a 1.6 nm band width monochromator tuned close to P11 band head of transitions from the excited level that is different from that used for the excitation. In particular, for the LIF measurements of levels $v = 0$, 5, 7 of $N_2(A)$, the excitation of (4,0), (8,5), (10,7) bands of FPS and detection of (4,1), (8,4) and (10,6) bands have been respectively used. Rhodamine 640, and DCM dyes have been used. The laser induced fluorescence pulses have been recovered by a fast transient digitising O-scope, and each pulse has been numerically integrated over a proper time interval. Care has been taken to avoid the residual scattered laser light. This latter, usually is removed by optical cut-off filter except for the cases when the detected emission arises from bands at lower wavelength than the laser one as is the case of fluorescence from (8,4) and (10,6) band. However, since scattered laser light vanishes after few tens of nanosecond in the fluorescence pulse, it is easy to exclude it by a proper choice of the integration gate. The photomultiplier has been gated to avoid non-linear effect when plasma induced emission is particularly strong [1].

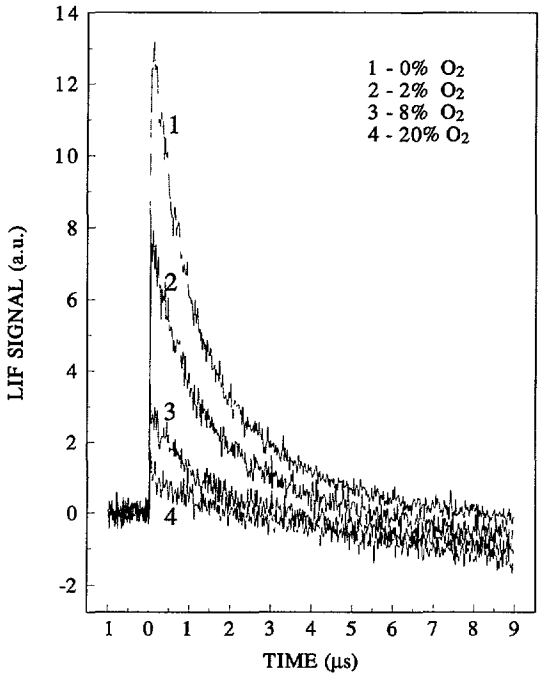

Fig. 2. — LIF pulses for $N_2(A, v = 0 - B, v' = 4 - A, v = 1)$ excitation-detection in N_2, and N_2 containing 2%, 8% and 20% O_2. Such pulse have only partially been elaborated. The zero is fixed to the beginning of the pulse. The baseline drift due to background emission decay has not been corrected (see text).

Typical LIF pulses in N_2/O_2 at the very early time in the afterglow are shown in Figure 2. The analysis of the decaying part of some of these pulses, reveals that in N_2 discharges, in general, the decay rate is pressure dependent and shows a two (or three) - exponential character. This indicates that the relaxation of the (B, v) state produced by the laser does not occur by a simple quenching mechanism but involves energy transfers with coupled electronic states [13–15]. Investigation of these aspects is actually in due course and will be accounted for in a forthcoming paper. Here we only remark that by the present excitation-detection facilities, the fast component of the decay can be carefully measured and will offer useful details about the $N_2(B, v)$ electronic state relaxation.

At low pressure, as in the present experiments, we have found that the decay in LIF pulse, for all the mixtures considered, is close to a single exponential. Therefore, the relaxation of the excited (B, v) state at this pressure can be seen as governed by a simple loss process, and this allows to correlate in first approximation the LIF signal to the $N_2(A)$ density by a simple expression:

$$I_{LIF} = \alpha K_P [N_2(A)] K_R / (K_R + K_Q) \quad (1)$$

where I_{LIF} is the integrated fluorescence, K_P is the laser pumping rate, K_R and K_Q are the radiative and collisional quenching rates respectively, and α is the optical efficiency of the apparatus. The K_Q value can be inferred from the fluorescence pulse. Expression (1) is no longer valid when the relaxation is markedly non exponential as in the case of a strong collisional coupling or when the problems related to the laser polarisation and the excitation-

detection geometry of the experiments are important, as we discussed in references [2] and [16]. In such cases a detailed model of the relaxation is required. On the other hand, we observed in [16] that single rotational excitation-detection condition is necessary for absolute density measurements by LIF. This condition is not realized in the present experiments thus here we will be concerned to only $N_2(A, v)$ relative densities.

The LIF signal grows on a plasma induced emission background whose contribution has to be removed from the pulse intensity. In the case of afterglow experiments, the background radiation is decaying and this affects the baseline of the pulses in the early afterglow, particularly when the LIF signal is weak, *i.e.* at high O_2 addition (see Fig. 2). We have subtracted the background by approximating it to a straight line fitting the beginning and the far end of the LIF pulse. Under this approximation we have found that the decay rate of LIF pulse is not much affected by the O_2 addition in N_2 feed at least for O_2 up to 15%. Thus for relative measurements of $N_2(A)$ density, the dependence of I_{LIF} on the quenching rate K_Q in equation (1) has been neglected.

2.2.2. NO($X^2\Pi$) *Detection.* — A favourable detection of NO(X) occurs *via* excitation-detection of NO-γ band systems ($A^2\Sigma - X^2\Pi$). In particular for the NO(X, $v = 0$) detection we use the excitation of (0,0) NO-γ band transition by laser photons at $\lambda_L = 226$ nm and detection of fluorescence from the (0,1) band, that is one of the strongest bands of $v = 0$ progression. The production of this UV photons is achieved by pumping rhodamine 590 dye by the second harmonic of Nd-Yag, and mixing the doubled dye beam with the Nd-Yag fundamental beam at 1.06 μm. BBO crystals have been used for second harmonic generation and mixing. Typical available energy at this wavelength is 200 μJ, that is sufficient for this experiments.

LIF measurement of NO formed in N_2/O_2 has been calibrated by NO in cell experiment carried out in the chamber. No effect of additive gases on the quenching of NO fluorescence state has been observed. The fluorescence pulse shape in the case of pure NO, or N_2/O_2/NO mixture in cell does not differ from that obtained when NO is formed by reaction in N_2/O_2 plasma at the pressure of our concern. Typical LIF pulses obtained on NO in cell and on NO formed in $N_2 + 5\%O_2$ experiment at 0.1 Torr are shown in Figure 3. In both cases we have verified that the decay part can be fitted by an single exponential whose time constant of 200 ns corresponds to the radiative lifetime of the NO(A,0) state.

2.2.3. NO-γ *Band Detection.* — Plasma induced emission of (0,3) NO-γ band has been measured also by fast transient digitising O-scope during the discharge pulse. Typical pulses are shown in Figure 4 at 0.1 Torr, several gas mixtures. For a careful analysis of the decay in post discharge, however, we have found more convenient the use of a photon counter detection that allows a larger dynamic range with respect to the digitising O-scope. By photon counter we have obtained four order dynamic range (see Fig. 12 in the following).

2.2.4. EEDF Measurement. — The electron energy distribution function has been measured in a cw N_2/O_2 discharge with one electrode capacitively coupled to the power supply and the other to ground (asymmetric configuration). The approach employed for minimising rf oscillation has been described in [2] and [17]. In the present measure a repetitive sweeping voltage has been applied to the probe in order to recover a full probe characteristics by the digitising O-scope. Such an approach is less accurate in recovering the EEDF close to the plasma potential than the technique applied in [17], that employed a triple probe scheme. It is on the other hand, faster and simpler, and offers, by virtue of the large number of equally spaced sampling points, the room for an heavier and easier application of numerical filters. The results are, then, sufficiently accurate for evidencing the main effects of O_2 addition to N_2 on EEDF.

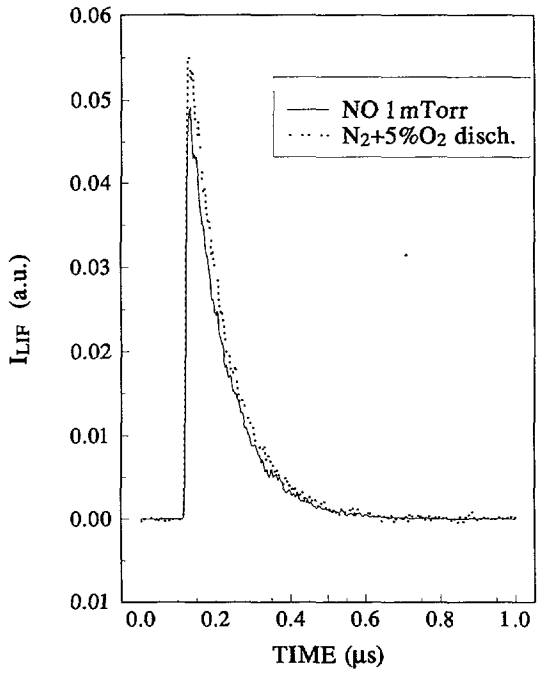

Fig. 3. — LIF pulses of NO(X, v = 0− A, v' = 0−A, v = 3) excitation-detection on NO in cell experiment and on NO formed in N_2+ 5% O_2 pulsed discharge.

3. Results and Discussion

3.1. About Electrons. — The electron distribution functions in pure nitrogen discharge and in N_2 containing few percent of O_2 are shown in Figure 5. Addition of O_2 reduces significantly the density of low energy (bulk) electrons, while fast electrons are only slightly reduced. Such a behaviour could be qualitatively explained by the high electron attachment rate of oxygen species. As a consequence, the excitation processes involving fast electrons, such as the electronic state excitation, will be less affected than the vibrational excitation of $N_2(X)$. A corroboration to probe results is shown in Figure 6, where the intensity of (0,2) band of N_2 Second Positive emission (SPS), that arises from $N_2(C^3\Pi_u)$ state at about 11 eV, normalized to N_2 partial pressure, has been reported as a function of O_2 content in the mixture. This state, in the discharge and in very early afterglow, is mainly excited by electron impact from $N_2(X, v)$ molecules [18]. We have measured by photon counter the decay of (0,2) SPS band for the different N_2/O_2 mixture and we found that the nature of the decay in post discharge observed in pure N_2 was practically unaffected by O_2 addition. This is an indication that O_2 does not modify the N_2(SPS) excitation mechanisms and the electron impact still remains the predominant mechanism in discharge. Therefore this emission, normalised to N_2 partial pressure, according to Actinometry [19] monitors the variation of the electron excitation efficiency by fast electrons (energy higher than 11 eV) as the mixture composition is changed. From Figure 6 we see that a small O_2 addition, about 1%, drops the efficiency by about a factor two. Then a decline of about 30% takes place for O_2 addition up to 20% in the feeding mixture.

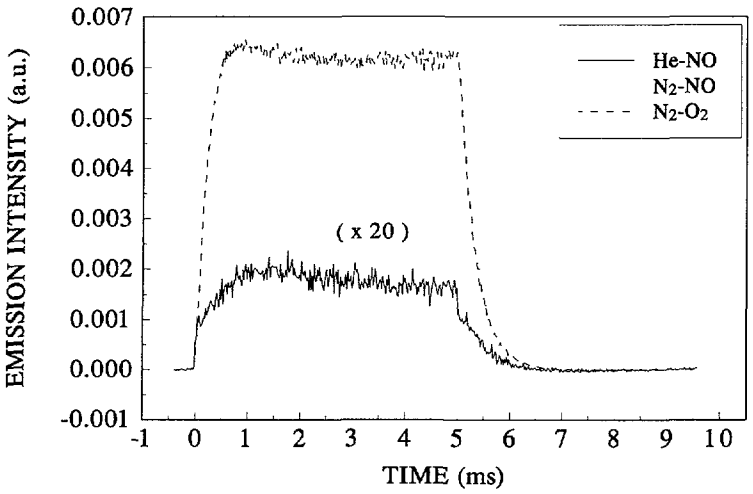

Fig. 4. — NO(0.3) γ band excitation during the pulsing at 0.1 Torr in N_2 + 1% O_2 N_2 – 1% NO discharge and He-1% NO.

3.2. $N_2(A^3\Sigma_u^+, v)$. — The decay of $N_2(A, v = 0, 5, 7)$ in pure N_2 post-discharge at 0.1 Torr and 5 ms pulsing is shown in Figure 7. In the case of $v = 0$, it is almost single exponential. Levels $v = 5$ and $v = 7$ decay with more complex pattern and can be fitted by two-three exponential laws. A quantitative inspection of this decay is beyond the scope of the paper. We want, however, to recall some important points in the following. In [12] we explained the multi-exponential decay of level $v = 4$ as due to the quenching by $N_2(X, v)$ molecules that in turn are quenched during the post discharge time. It was also shown that the higher the vibrational temperature or non Boltzmann character of $N_2(X, v)$ distribution, the higher the quenching rate. In this collision, $N_2(X, v)$ molecule is excited to $N_2(B^3\Pi_g)$ state by energy transfer from the metastable. This mechanism depopulates more favourably the higher levels of A state than the lower ones. This is because (A, $v = 0$) transfers energy to $N_2(X, v \geq 5)$ molecules for the (B, v) state excitation [20], while (A,4) to $N_2(X, v \geq 2)$ molecules [12] whose density is clearly higher. This explanation could be still valid for levels 5 and 7. In particular, level (A,7) is resonant with (B,0) so that it is strongly coupled by collision with N_2, as discussed by many authors [13–15]. The effectiveness of further quenching mechanisms of A state involving N atoms and (A + A) pooling reactions exciting $C^3\Pi_u$ were also examined. Although the relaxation of $N_2(C, v)$ distributions confirmed the high efficacy of the pooling excitation mechanisms [18] in post discharge, the rate of this process cannot give account of the loss of N_2 (A). At the end, we must underline that the modelling of the relaxation of measured ($B^3\Pi_g$, v) distribution in [3] evidenced some conflict with the use of the current overall rate coefficient of [20] for $N_2(A, v)$ +$N_2(X, v)$ processes producing $N_2(B, v)$ states. This was due to an erroneous scaling of this experimental rate coefficient to the calculated state to state energy gap rate coefficients used in (B, v) simulation. The correct scaling reveals that e + $N_2(A, v)$ process by low energy electrons can compete with (X + A) process in (B, v) excitation. To this concern a more accurate analysis of the whole $N_2(A, v)$ distribution relaxation is probably necessary.

When O_2 is added to N_2 discharges, the N_2(A,0) quenching rate significantly rise, as can be seen in Figure 8, where the decays of level N_2(A,0) at different O_2 percentage in 0.1 Torr

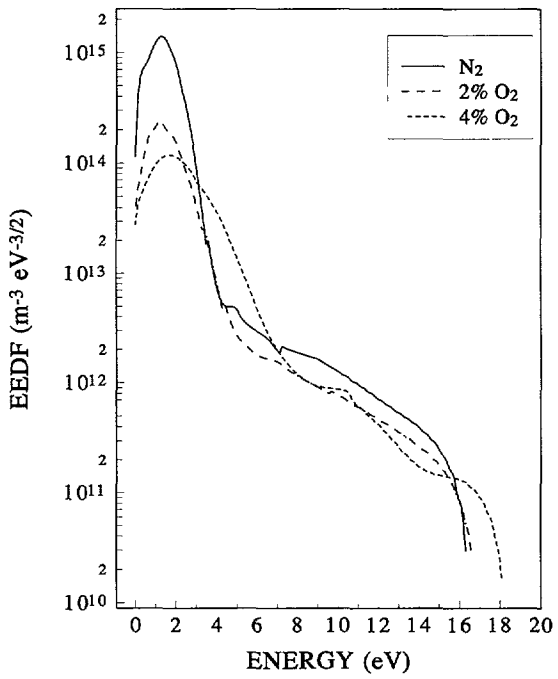

Fig. 5. — EEDF measured in cw rf discharges at 0.1 Torr for N_2 and mixtures containing 2% and 4% of O_2.

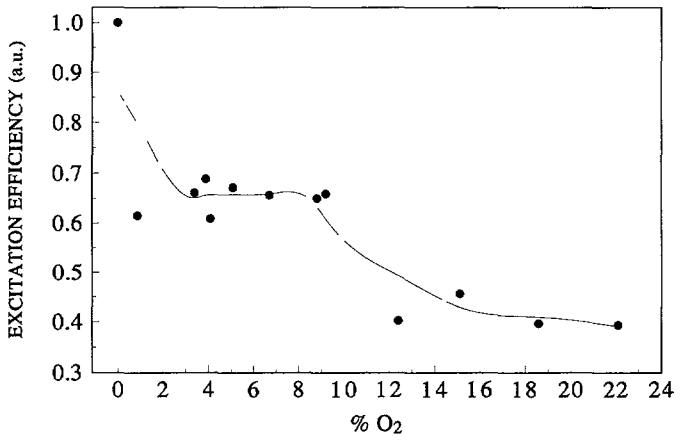

Fig. 6. — Electron excitation efficiency (Actinometry) by fast electrons of $N_2(0,2)$ SPS band.

discharge have been reported. The decay maintains a single exponential form within a large dynamic range. Some considerations about the quenching mechanisms of $N_2(A,0)$ state will be given in Paragraph 3.5.

The integrated I_{LIF} signal, at the end of the discharge pulse as function of the O_2 percentage is shown in Figure 9. This curve, as discussed in Paragraph 2.2.1, represents in first approximation, the relative density of $N_2(A,0)$ metastable. The density of $N_2(A,0)$ in air like mixture is more than one order of magnitude lower than in N_2 discharges.

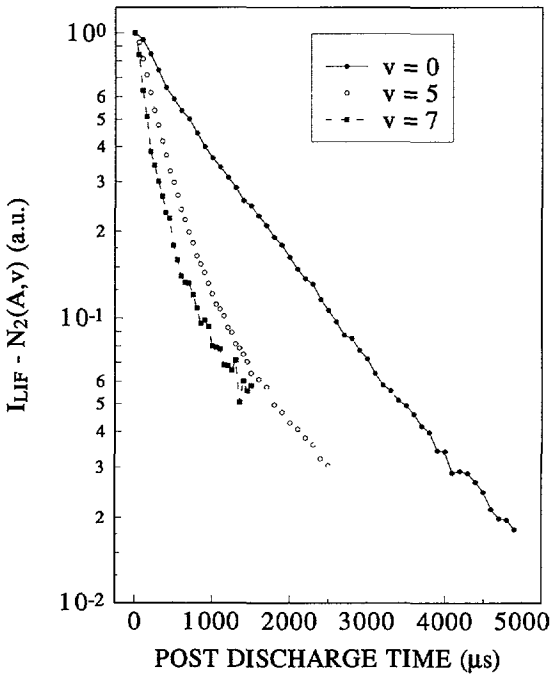

Fig. 7. — Decays of N_2(A, $v = 0$, 5, 7) in N_2 post discharge at 0.1 Torr 100 Hz pulsing.

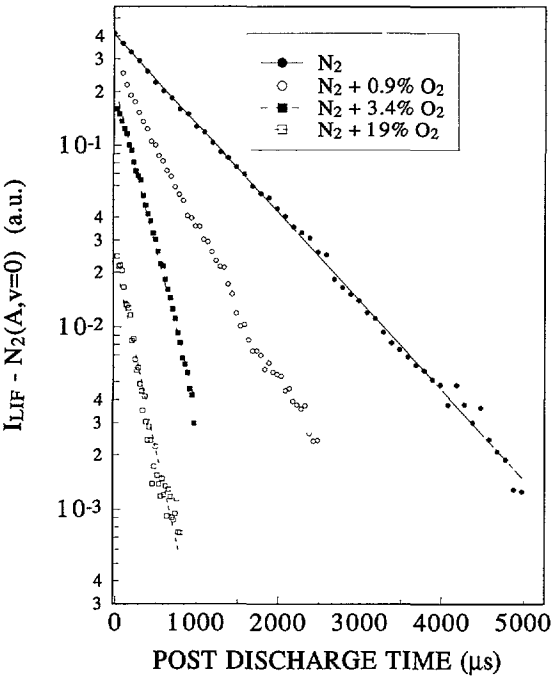

Fig. 8. — Decays of N_2(A, $v = 0$) at various % O_2 at 0.1 Torr.

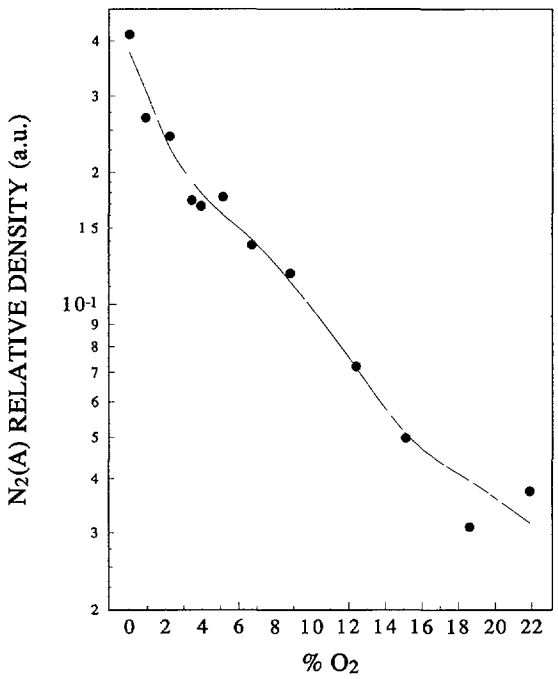

Fig. 9. — Relative density of $N_2(A, v = 0)$ as a function of % O_2.

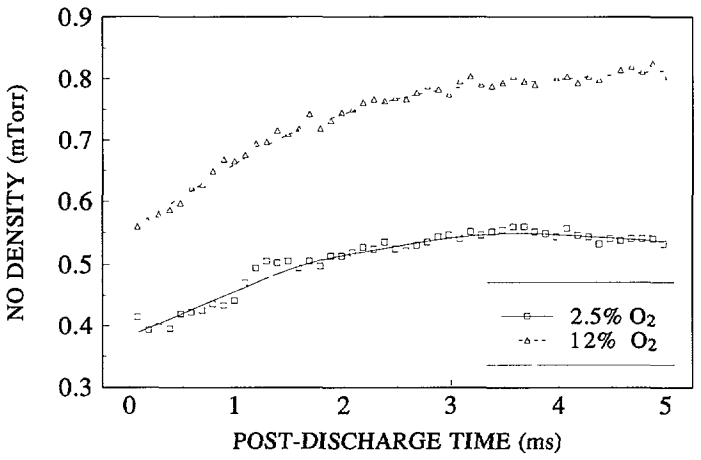

Fig. 10. — NO density in N_2/O_2 during the post discharge time.

3.3. $NO(X^2\Pi)$. — The measured NO density in N_2 post-discharge containing 2.5 and 12% O_2 at 0.1 Torr at 100 Hz repetition rate and 50% duty cycle, are shown in Figure 10. NO density increases in post-discharge and decreases during the discharge regime by the same amount. The residence time of the species in the electrode gap is difficult to estimate. For a flow rate of 80 sccm, the volume of the plasma chamber is replenish after about 80 ms. Therefore feeding gases "see" several discharge pulses before being pumped out the discharge gap. For repetitive excitation pulses NO density is established in the reactor. The decreasing of NO in

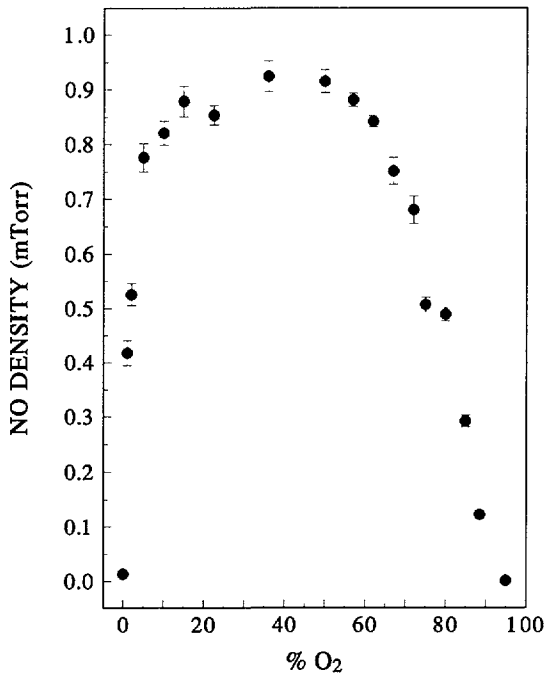

Fig. 11. — NO density in cw rf discharge at 0.1 Torr as function of O_2.

discharge, and the increasing in post-discharge, that take place in a millisecond time scale, are probably due to dissociation and recombination processes, the analysis of which requires further investigations. The NO degree of dissociation amounts to about 40%. A similar behaviour is also observed in discharges fed with N_2 - 1%NO and in He- 1%NO mixtures.

The NO(X) density, measured by LIF in a cw discharge, as a function of O_2 percentage is shown in Figure 11. NO goes through a maximum at about 40% O_2 and the curve is to some extent asymmetric. The production rises steeply for O_2 percentage up to 20% . The maximum formation yield is at about 1% O_2 in the mixture.

3.4. NO($A^2\Sigma$). — The time evolution of (0,3) NO-γ band measured by TRPIES during the pulsing in N_2 containing 2.5% O_2 at 0.1 Torr, has been shown in Figure 4. The rise of γ band to the steady state value in the pulse takes place in about 0.5 ms. The decay of this band has been examined in detail at various O_2 addition, and for all the conditions it is almost single exponential, as shown in Figure 12. The main point of these measurements is that, contrary to electronic state excitation of other species, no fast component due to electron relaxation is observed at low pressure.

In order to elucidate this point we also have measured the excitation of (0,3) γ band in N_2 + 1%NO and He + 1%NO mixtures (see Fig. 4). We have observed fast excitation and de-excitation components only in the case of He mixture, as can be clearly seen in Figure 13 where particulars of normalized decay curves have been reported. Moreover, the γ band excitation in mixtures containing N_2 is much stronger than in He case. This fast process is associated to electron impact NO-γ system excitation from NO(X). The energetic electrons (higher than 5.4 eV, that is the threshold of X-A excitation) in fact relax in a microsecond time scale, as we showed in [21] for He-N_2 discharges. The lack of this fast component in N_2-NO mixtures

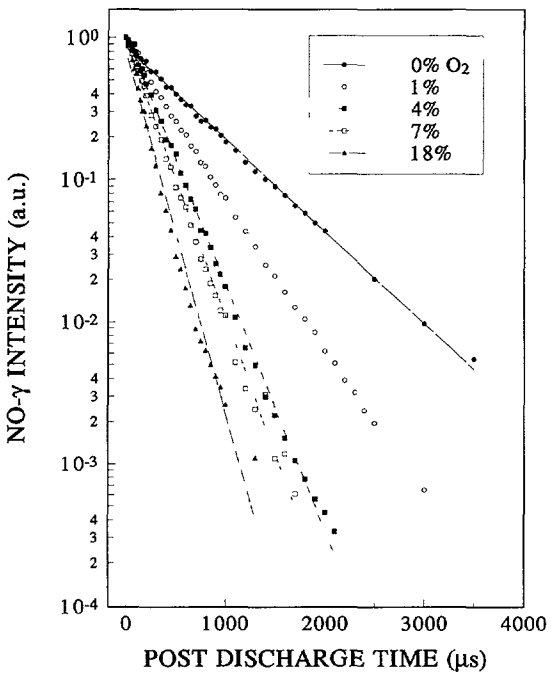

Fig. 12. — Decay of (0,3) NO-γ band in post discharge at various O_2 percentages.

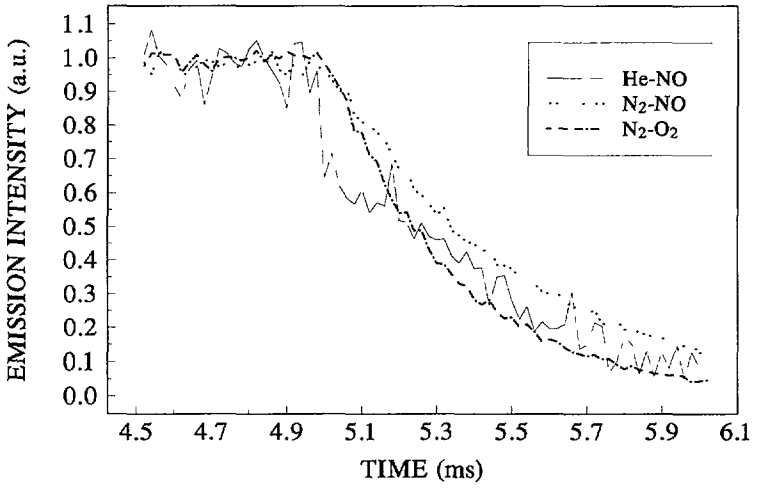

Fig. 13. — Particulars of normalized NO(0,3) γ decay curves for different mixture. The discharge switching OFF time is 5 ms.

indicates that the electron impact excitation is negligible with respect to other mechanisms involving excited N_2.

The NO-γ bands excitation by N_2 (A) - NO collisions has been studied by several authors [22], and state to state rates for N_2(A) vibrational levels have been also proposed. It was found

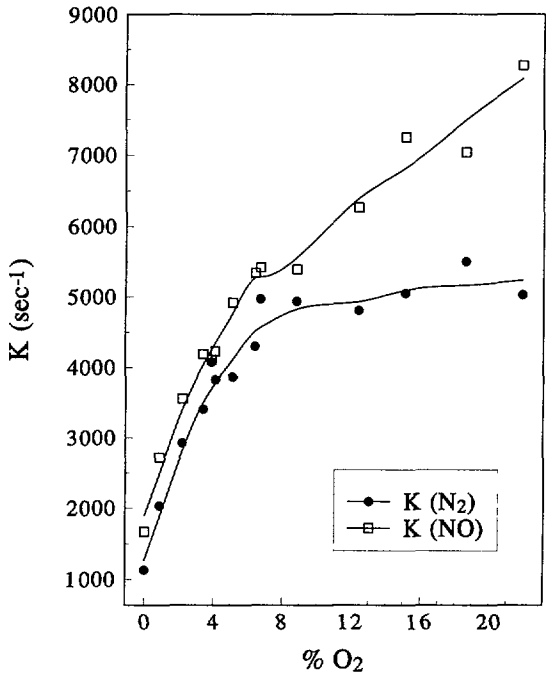

Fig. 14. — Quenching rates of NO(A, $v = 0$) and N_2(A, $v = 0$) *vs.* % O_2.

that in collisions NO(A, $v = 0$) is excited by N_2(A, $v = 0$, 1, 2), while the quenching of N_2(A, $v = 0$) results mainly in NO(A, $v = 0$). A correlation between the decay of N_2(A,0) and that of NO(A,0) is then to be expected. This is qualitatively shown in Figure 14 where the decay rates of (0,3) NO-γ and N_2(A,0) have been plotted as a function of % O_2 in the feeding mixture. The quenching rate of NO(A,0) follows that of N_2(A,0) although its value is always higher. A significant deviation in the trend appears for O_2 percentages higher than 10% where NO(A,0) rate is still increasing while that of N_2(A,0) almost saturates. At the present we do not have an exhaustive explanation for such a deviation. However, one should consider that N_2(A, $v = 1$ and 2) molecules also contribute to the NO(A,0) excitation [22]. The quenching of these states by oxygen is faster than that of $v = 0$ but comparable to it [23–25]. This would produce a multi-exponential decay of NO-γ band which is not clearly recognised because of the similar decay time constants so that it looks like as a single exponential with an "averaged" faster time constant. Weak deviations from single exponential decay are recognisable for O_2 higher than 10% (see Fig. 12), but further work is necessary to fully elucidate this aspects.

3.5. QUENCHING OF N_2(A, $v = 0$) AND O_2 DISSOCIATION. — From the considerations developed in Section 3.2, the single exponential decay of (A, $v = 0$) level measured in N_2 discharge must be predominately attributed to a diffusion loss to the reactor wall that at 0.1 Torr was estimated to be about 740 s^{-1} [12]. The measured values under the present conditions is 1130 s^{-1} Such a difference can be reasonably attributed to a quenching by N atoms, as we discuss in [12], and by a leak of oxygen impurities. This latter contribution is negligible since we measure about 0.02 mTorr of NO in a "pure" N_2 conditions. The N density is then estimated to be about 8×10^{12} cm^{-3}, using a quenching rate coefficients of 4×10^{-11} cm^3 s^{-1} (see Ref. [12]). This corresponds to nitrogen dissociation degree of about 0.2%. Addition of

O_2 to the mixture strongly enhances the quenching rate. First, on the basis of EEDF results, we observe that O_2 addition, even in small amount, lowers the vibrational excitation of $N_2(X)$, because of the lowering of bulk electron density. This rules out any contribution to the quenching by $N_2(X, v)$ collisions. The most important $N_2(A)$ quenching processes, when oxygen is added to N_2 discharge, are the following:

$$N_2(A, v) + O(^3P) \rightarrow NO(X, v) + N(^4S) \tag{2a}$$

$$N_2(A, v) + O(^3P) \rightarrow NO(X, v) + N(^2D) \tag{2b}$$

$$N_2(A, v) + O(^3P) \rightarrow N_2(X, v) + O \tag{3}$$

$$N_2(A, v) + O_2 \rightarrow NO_2, NO, N_2(X, v), O \tag{4}$$

$$N_2(A, v) + NO \rightarrow NO(A^2\Sigma, v) + N_2. \tag{5}$$

These mechanisms have been studied by several authors [22–27]. On the basis of the data of Figures 11 and 14 and of the rate coefficients from literature, we can infer under proper assumptions the O atomic density and the O_2 dissociation degree for the various mixture investigated.

The measured quenching rate can be approximated by:

$$K = K_D + K_{NO} + K_O + K_{O_2}. \tag{6}$$

The contribution by diffusion is unchanged when O_2 is added to the mixture. The contribution by NO, process (5), can be estimated from the data of Figure 11 and the rate coefficient measured in [22], that is about 6.6×10^{-11} cm^3 s^{-1}. Using the quenching rate coefficients values of 3×10^{-11} cm^3 s^{-1} [23] as overall rate coefficient of processes (2) and (3), and of 2×10^{-12} cm^3 s^{-1} [24] for process (4) and balancing O_2 loss by O, and NO products we calculate the O_2 dissociation degree and the O density from the measured K values of Figure 14. We have neglected N_2O in the O_2 loss balance on the basis of branching ratios measured in [26]. On the other hand, the formation of N_2O by O_2 reaction with $N_2(X, v > 15)$ [27] is negligible because of the low vibrational excitation of N_2 [12, 18]. The results of O_2 dissociation degree and of O density at the various O_2 percentages are reported in Figure 15. The O density profile presents a maximum displaced towards the low O_2 percentages, and the O_2 dissociation degree decreases from 40% to 4% as O_2 addition is increased up to 22%.

Concluding Remarks

The present results address some aspects of N_2/O_2 discharge kinetics. A complete picture of this complex kinetics would require measurements, possibly direct, of further species like O, N, N_2O and $N_2(X, v)$ molecules as well as the amount of N_2 and O_2 during the pulsing. LIF and CARS measurements will be implemented to achieve such goals. At present we remark the main results obtained by the present diagnostics:

a) NO-γ band in N_2/O_2 plasma are predominantly produced by collisions with $N_2(A)$ metastable.

b) NO and O profiles with a maximum as a function of O_2 percentages in the feed are very similar to that measured by mass spectrometry and actinometry in flowing dc discharge in Pyrex reactors [5]. Such a kind of profile has been attributed in [28] to wall reactions of N, O, and NO.

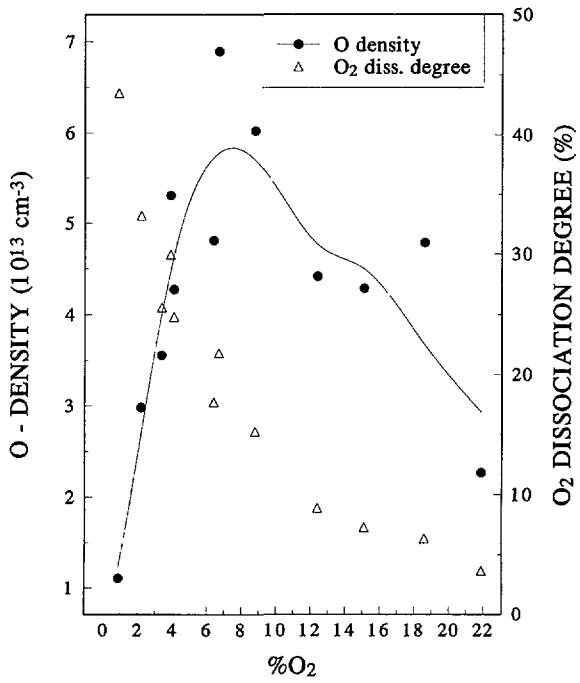

Fig. 15. — Trends of O density and O_2 dissociation yield *vs.* % O_2.

c) The quenching of $N_2(A, v = 0)$ can reasonably be accounted for by an important contribution by O atoms.

Finally we want to stress the importance of LIF spectroscopy for measuring $N_2(A, v)$ relaxation in N_2/O_2 plasmas. This technique even though difficult to calibrate for absolute density measurements overcomes the problems of standard Vegard Kaplan emission analysis, coming from overlapping with strong NO-γ band and N_2 second positive emissions [18]. Preliminary results on the quenching of different vibrational levels of $N_2(A, v)$ indicate that up to 9 levels are accessible by LIF in N_2/O_2 mixture. In addition, the analysis of N_2(A-B) laser fluorescence pulse with short pulsed dye laser and fast transient digitising O-scope allows to study the fast components of $N_2(B, v)$ relaxation that contain information on the coupling of (B, v) with the neighbouring $W^3\Delta$, and $B'^3\Sigma_u$ electronic states.

Acknowledgments

This work has been partially supported by the Italian Space Agency (ASI).

References

[1] De Benedictis S. and Dilecce G., *Plasma Source Sci. Technol.* **4** (1995) 212.
[2] De Benedictis S. and Dilecce G., *J. Phys. D: Appl. Phys.* **28** (1995) 2067.
[3] De Benedictis S., Dilecce G., Simek M. and Cacciatore M., Proc. ISPC-12, Minneapolis, J.V. Eberlein, D.W. Ernie, J.T. Roberts, Eds., vol. 1 (1995) pp. 415.

[4] Kossyi A., Kostinsky A.Yu., Matveryer A.A. and Silakov V.P., *Plasma Source Sci. Technol.* **1** (1992) 207.
[5] Nahorny J., Ferreira C.M., Gordiets B., Pagnon D., Touzeau M. and Vialle M., *J. Phys. D: Appl. Phys.* **28** (1995) 738.
[6] Guerra V. and Loureiro J., *J.Phys. D: Appl. Phys.* **28** (1995) 1903.
[7] Doroshenko V.M., Kudryatvsev N.N. and Smetanin V.V., *High Temp.* **29** (1991) 815.
[8] Zipf E.C., *Nature* **287** (1983) 523.
[9] Armenise I., Capitelli M., Colonna G., Koudriatvsev N. and Smetanin V., *Plasma Chem. Plasma Process.* **15** (1995) 501.
[10] M. Capitelli, Ed. in "Molecular Physics and Hypersonic flows" NATO-ASI, Vol. C-482 (Kluer Academic Publishers, 1996).
[11] Yasuda Y., Zaima S., Kaida T. and Koide Y., *J. Appl. Phys.* **67** (1990) 2603.
[12] De Benedictis S., Dilecce G. and Simek M., *Chem. Phys.* **178** (1993) 547.
[13] Sadeghi N. and Setser D.W., *J. Chem. Phys.* **15** (1983) 2710.
[14] Rotem A. and Rosenwaks S., *Optical Eng.* **22** (1983) 564.
[15] Bachmann R., Li X., Oettinger Ch., Vilesov A.F. and Wulfmeyer V., *J. Chem. Phys.* **98** (1993) 8606.
[16] Simek M., Dilecce G. and De Benedictis S., *Plasma Chem. Plasma Process* **15** (1995) 427.
[17] Dilecce G., Capitelli M. and De Benedictis S., *J. Appl. Phys.* **69** (1991) 121.
[18] De Benedictis S. and Dilecce G., *Chem. Phys.* **192** (1995) 149.
[19] De Benedictis S., Dilecce G. and Gorse C., *Plasma Chem. Plasma Process* **11** (1991) 335.
[20] Piper L.G., *J. Chem. Phys.* **88** (1988) 231.
[21] Dilecce G. and De Benedictis S., *Plasma Source Sci. Technol.* **2** (1993) 119.
[22] Piper L.G., Cowles L.M. and Rawlins W.T., *J. Chem. Phys.* **85** (1986) 3369.
[23] Piper L.G., Caledonia G.E. and Keannely J.P., *J. Chem. Phys.* **75** (1981) 2847.
[24] Piper L.G., Caledonia G.E. and Keannely J.P., *J. Chem. Phys.* **74** (1981) 2888.
[25] De Sousa A.R., Touzeau M. and Petitdidier M., *Chem. Phys. Lett.* **121** (1985) 423.
[26] Fraser M. and Piper L.G., *J. Phys. Chem.* **93** (1989) 1107.
[27] Fraser M., Tuker T.R., Piper L.G. and Rawlins W.T., *J. Geophys. Res.* **95** (1990) 18-611.
[28] Gordiets B., Ferreira C.M., Guerra V., Loureiro J., Nahorny J., Pagnon D., Touzeau M. and Vialle M., *IEEE Trans. Plasma Sci.* **23** (1995) 750.